2020-01-2243

Slip speed and drive torque planning of multivariable controller for an electrified vehicle with dual clutch transmission

Dong-Hyun Kim and Seibum B. Choi
Korea Advanced Institute of Science and Technology, Republic of Korea

Abstract

Demand for electrified vehicles is increasing due to increased environmental pollution regulations and interest in highly efficient vehicles. According to these demands, research on electrified vehicles equipped with Dual Clutch Transmission (DCT) has been actively conducted for the purpose of improving energy efficiency of electrified powertrain, maximizing acceleration performance, and increasing maximum speed. However, since DCT requires clutch to clutch shifting, it is difficult to control drive torque and slip speed using two clutch actuators and a power source input. In order to solve this, a study on a multivariable shift controller has been conducted. However, this study chose a heuristic planning method to control the two outputs. However, since the slip speed and drive torque are coupled, it is necessary to tune the reference for every shift scenario, as well as create unnecessary control inputs or degrade shift control performance. Therefore, this study proposes a reference planning method considering powertrain dynamics. Specifically, by using the powertrain modeling of the electrified vehicle, a reference composed of power source input, slip speed, and drive torque can be constructed while satisfying dynamics. Using the proposed method, the slip speed is uniquely determined when the reduction ratio of the power source torque and the inertia phase time are predetermined. In order to verify the proposed planning method in this paper, an electrified powertrain simulator designed with a multivariable controller was constructed with MATLAB / SIMULINK. Afterwards, the heuristic reference planning method of the previous study and the method proposed in this paper were simulated in a vehicle composed of the same shift controller and powertrain. As a result, not only the reference automatically generated without tuning, but the energy consumption of the clutch actuator is reduced by about 10% in the control result with the same ride quality.

Introduction

Demand for vehicles with high energy efficiency is increasing as environmental pollution regulations are strengthened and interest in high-efficiency vehicles is increasing. In response to these demands, sales of Hybrid Electric Vehicles (HEV) and Electric Vehicles (EV) which are motor-powered vehicles are increasing. Both HEV and EV use a driving motor as a power source, so it can be called an electrified vehicle. In particular, HEV can be divided into parallel and series according to the role of the internal combustion engine (ICE). In addition, both the parallel HEV where the motor and ICE generate driving torque together and the series HEV where the ICE generates electricity to charge the battery have a common thing: they use the motor as a power source. This commonality has the advantage of being able to intervene in powertrain control due to the quick response of the power source, unlike vehicles driven only by ICE.

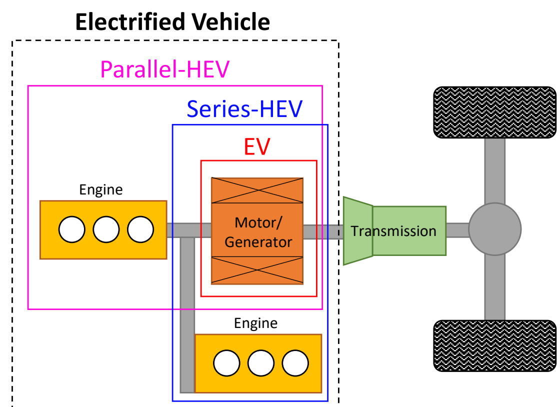

Figure 1: Powertrain of various types of electrified vehicles. Parallel HEV, series HEV, EV are all commonly used as a power source, so they are responsive enough to be used as a control input.

Using these advantages, electrified powertrain equipped with various transmissions has been studied for the purpose of improving energy efficiency, maximizing acceleration performance, and increasing maximum speed [1–10]. Among them, research has been actively conducted on electrified vehicles equipped with Dual Clutch Transmission (DCT) that can maximize acceleration performance and energy efficiency by using clutch to clutch shift [1–5]. Representatively, there are studies on a system in which a DCT is installed in a parallel HEV [3–5] or a 2-speed DCT is installed in an EV [1–3]. However, since DCT requires clutch to clutch shifting, the drive torque and slip speed must be controlled using two clutch actuators and a power source. Therefore, it is difficult to control because it is a multi-input multi-output (MIMO) system and the input and output are decoupled from each other.

To simplify this problem, the shift state can be divided into three phases and a control strategy can be established for each phase. The torque phase from which the torque is transmitted from the off-going clutch to the on-coming clutch, the inertia phase synchronizing the speed between the on-coming clutch and the power source, the end phase where vibration occurs due to the difference in friction coefficient when the engagement of the on-coming clutch is completed are three phases of the DCT shift. Torque phase is generally very short, and it is known that it is important to match the disengage timing of the off-going clutch [5]. Therefore, through the open loop control, the clutch is completely disengaged when the torque of the off-going clutch becomes $0Nm$. In the end phase, lock-up oscillation occurs due to the difference between slip torque and engagement torque, which can be improved by matching the slip torque and engagement torque in the inertia phase. Therefore, in this paper, the disengage timing of the off-going clutch is adjusted with the open loop controller in the torque phase, and the closed torque controller is used in the inertia phase to control the drive torque to minimize lock-up oscillation in the end phase.

However, in the inertia phase of electrified vehicles, drive torque and slip speed must be controlled using on-coming clutch torque and power source torque. However, since both inputs are coupled to outputs, they cannot be controlled by a single input single output (SISO) controller. To solve this difficulty, there is a study in which two outputs are decoupled through a multivariable shift controller [5]. However, the reference for controlling the two outputs was selected heuristically. Specifically, inertia phase time (t_{ip}) is determined according to the pedal position or driving mode of the driver, and maximum drive toque ($T_{o,max}$) is determined according to the initial torque of each shift. In addition, the shape of each reference is determined based on the sinusoidal function. The algorithm proposed in this paper is shown in Fig. 2.

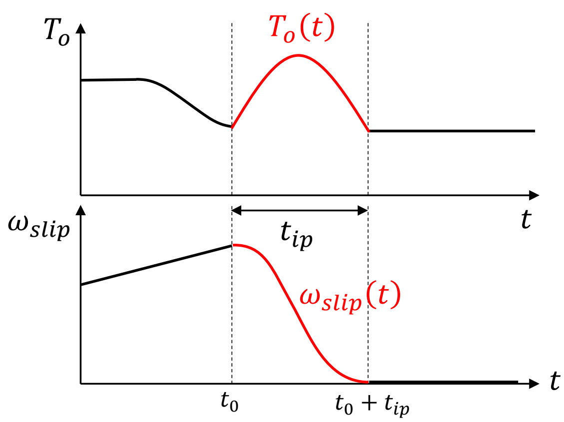

Figure 2: Reference planning method of slip speed and drive torque proposed in previous research [5]. Each reference is independently based on a sinusoidal function.

However, although the references to the two outputs were independently generated, the relationship between the initial torque ($T_o(t_0)$) and ($T_{o,max}$) was unclear, requiring tuning in various shift scenarios. In addition, since the relationship between slip speed and drive torque is unclear, unnecessary input may be generated or control results may be deteriorated.

Therefore, this study proposes a reference planning method for slip speed and drive torque for DCT shift control of electrified vehicles using multivariable controllers. Through the proposed method, it is possible to minimize the effort for tuning by automatically generating a reference. Additionally, unnecessary control inputs can be eliminated and shift control performance and stability can be improved. Section 2 models the powertrain of an electrified vehicle equipped with DCT, and Section 3 proposes a reference planning method using powertrain dynamics. In Section 4, a multivariable controller to which the proposed method is applied is designed and verified through simulation in Section 5. Finally, this study is concluded in Section 6.

Target system modeling

The powertrain of the electrified vehicle equipped with DCT can be modeled as the following equation using the Fig. 3 showing the inertia phase.

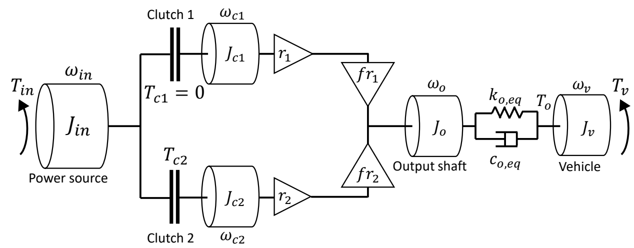

Figure 3: Free body diagram of electrified vehicle powertrain equipped with DCT.

$$J_{in}\dot{\omega}_{in} = T_{in} - T_{c2} \tag{1}$$

$$J_{c1}\dot{\omega}_{c1} = -\frac{r_2 fr_2}{r_1 fr_1}T_{c2} - \frac{1}{r_1 fr_1}T_o \tag{2}$$

$$J_{c2}\dot{\omega}_{c2} = T_{c2} - \frac{1}{r_2 fr_2}T_o \tag{3}$$

$$J_o\dot{\omega}_o = r_2 fr_2 T_{c2} - T_o \tag{4}$$

$$J_v\dot{\omega}_v = T_o - T_v \tag{5}$$

$$T_o = k_{o,eq}(\theta_o - \theta_v) + c_{o,eq}(\omega_o - \omega_v) \tag{6}$$

where, $in, c1, c2, o$ and v mean power source, clutch 1, clutch 2, output shaft and vehicle, respectively. In addition, J, T, ω and θ mean rotational inertia, torque, rotational speed and rotational angle of each component. r_1, r_2, fr_1 and fr_2 denote first gear, second gear, first final gear and second final gear ratio, respectively. $k_{o,eq}$ and $c_{o,eq}$ indicate the stiffness and damping coefficient of the output shaft. T_v represents road disturbance. In this model, the drive torque transmitted to the vehicle is expressed as the output shaft torque (T_o).

In equations (2) and (3), the inertia of clutch 1, 2 and output shaft are all expressed as equivalent inertia $J_{c2,eq}$, and the output shaft speed is expressed as clutch 2 speed, which is simplified to the equation with three states as follows.

$$\dot{\omega}_{in} - \dot{\omega}_{c2} = \frac{T_{in}}{J_{in}} - \Big(\frac{1}{J_{in}} + \frac{(r_2 fr_2)^2}{J_{c2,eq}}\Big)T_{c2} + \frac{r_2 fr_2}{J_{c2,eq}}T_o \tag{7}$$

$$\frac{\dot{\omega}_{c2}}{r_2 fr_2} - \dot{\omega}_v = -\Big(\frac{1}{J_{c2,eq}} + \frac{1}{J_v}\Big)T_o + \frac{r_2 fr_2}{J_{c2,eq}}T_{c2} + \frac{1}{J_v}T_v \tag{8}$$

$$\begin{aligned}\dot{T}_o = k_{o,eq}\Big(\frac{\omega_{c2}}{r_2 fr_2} - \omega_v\Big) - c_{o,eq}\Big(\frac{1}{J_{c2,eq}} + \frac{1}{J_v}\Big)T_o \\ + \frac{c_{o,eq} r_2 fr_2}{J_{c2,eq}}T_{c2} + \frac{c_{o,eq}}{J_v}T_v\end{aligned} \tag{9}$$

$$where, J_{c2,eq} = (r_2 fr_2)^2 J_{c2} + (r_1 fr_1)^2 J_{c1} + J_o \tag{10}$$

Reduced powertrain dynamics is expressed in the state-space form using slip speed ($\omega_{in} - \omega_{c2} = \omega_{slip}$), output shaft compliance rate ($\omega_o - \omega_v = \frac{\omega_{c2}}{r_2 fr_2} - \omega_v$), and drive torque ($T_o$) as the state and slip speed and drive torque as the output as the following equation.

$$\dot{\mathbf{x}} = \mathbf{A}\mathbf{x} + \mathbf{B}\mathbf{u} + \mathbf{E}\boldsymbol{\delta}$$

$$where, \mathbf{x} = \begin{bmatrix} \omega_{in} - \omega_{c2} \\ \frac{\omega_{c2}}{r_2 f r_2} - \omega_v \\ T_o \end{bmatrix}, \mathbf{u} = \begin{bmatrix} T_{in} \\ T_{c2} \end{bmatrix}, \boldsymbol{\delta} = T_v,$$

$$\mathbf{A} = \begin{bmatrix} 0 & 0 & \frac{r_2 f r_2}{J_{c2,eq}} \\ 0 & 0 & -\left(\frac{1}{J_{c2,eq}} + \frac{1}{J_v}\right) \\ 0 & k_{o,eq} & -c_{o,eq}\left(\frac{1}{J_{c2,eq}} + \frac{1}{J_v}\right) \end{bmatrix}, \mathbf{E} = \begin{bmatrix} 0 \\ \frac{1}{J_v} \\ \frac{c_{o,eq}}{J_v} \end{bmatrix},$$

$$\mathbf{B} = \begin{bmatrix} \frac{1}{J_{in}} & -\left(\frac{1}{J_{in}} + \frac{(r_2 f r_2)^2}{J_{c2,eq}}\right) \\ 0 & \frac{r_2 f r_2}{J_{c2,eq}} \\ 0 & \frac{c_{o,eq} r_2 f r_2}{J_{c2,eq}} \end{bmatrix} \tag{11}$$

Reference planning of control variable

Relationship between slip speed and drive torque

The relationship between slip speed and drive torque can be obtained from the dynamics of state 1 in equation (7) If the output shaft compliance effect is ignored in this equation, equation (7) is expressed as follows.

$$T_o = r_2 f r_2 T_{in} - J_{in} r_2 f r_2 \dot{\omega}_{slip} \tag{12}$$

It can be seen from equation (12) that the slip speed and drive torque are dependently determined by the power source input. Therefore, if two of the three variables are predetermined, the other must be determined based on the equation (12) to create the reference that satisfies the powertrain dynamics. For example, a reference of a drive torque (T_o) for evaluating shift quality and a feed forward input of a power source torque (T_{in}) considering input constraints can be planned using a sinusoidal shape. In this case, the slip speed reference can be planned through the following equation.

$$\omega_{slip}(t) = \int \left(\frac{T_{in}(t)}{J_{in}} - \frac{T_o(t)}{J_{in} r_2 f r_2}\right) dt \tag{13}$$

In this way, the reference of control variables can be planned considering the characteristics of the powertrain. Satisfying powertrain dynamics in this method prevents unnecessary control inputs from being generated and can suppress jerk. Therefore, it is possible to increase the performance and energy efficiency of the shift control.

Relationship between initial power source torque and maximum drive torque

The initial power source torque ($T_{in}(t_0)$) of the inertia phase may vary depending on the driver's torque demand or driving mode (sports, comfort). If the driver torque demand is high, the maximum drive torque ($T_{o,max}$) should be increased to increase the torque transmitted to the vehicle, and if it is small, it must be decreased. Therefore, it was necessary to tune the drive torque reference according to the driver torque demand. Not only does this tuning increase cost, it cannot always produce optimal drive torque planning. Therefore, in this paper, we propose an algorithm that can automatically calculate the maximum drive torque according to $T_{in}(t_0)$ using the powertrain dynamics.

The drive torque reference depends on the driving mode when the driver torque demand is the same. Therefore, the proposed method changes the maximum drive torque according to the driving mode when the driver torque demand is the same. For example, a sports mode that increases acceleration performance can maintain the power source torque at the same value as the initial value to transmit maximum torque during shifting, and the comfort mode that improves riding comfort can be reduce the torque transmitted to reduce jerk. Where, it is assumed that the power source torque during shifting cannot be greater than the initial value, which is the driver torque demand. It is possible to calculate T_{in} for maximum T_o using Equation (12), but it is more intuitive to calculate T_o through the reduction amount of T_{in} according to the driving mode by using $T_{in}(t_0)$ as the maximum value of T_{in}(Fig. 4). Therefore, the T_{in} reduction ratio according to a predetermined drive mode can be defined as η ($0 < \eta < 1$). When calculating the $T_{o,max}$ using η, the following equation can be used.

$$T_{o.max} = r_2 f r_2 (1 - \eta) T_{in}(t_0) - J_{in} r_2 f r_2 \max(\dot{\omega}_{slip}) \tag{14}$$

$T_{o,max}$ can be calculated by applying the following slip speed constraint to equation (14).

$$\int_{t_0}^{t_0 + t_{ip}} \dot{\omega}_{slip} dt = -\omega_{slip}(t_0) \tag{15}$$

$$T_{o.max} = f\big(\eta T_{in}(t_0), \omega_{slip}(t_0)\big), (0 < \eta < 1) \tag{16}$$

The η according to the driving mode can be selected as follows. The larger η reduces the torque of the power source, so jerk also decreases as the drive torque decreases. Therefore, when η is large (Fig. 4 (a)) can be selected as the comfort mode, and when η is small or 0 (Fig. 4 (b)) can be selected as the sports mode.

References generated through the proposed method are automatically generated as Fig. 5 if η and t_{ip} are determined according to driving mode. As shown in the figure, it can be seen that even if $T_{in}(t_0)$ is different, a reference is automatically generated. In addition, since the relations of the references are based on powertrain dynamics, unnecessary control inputs are not generated, and the effect of reducing jerk can be accompanied.

The feed forward input of the power source and clutch torque for tracking the reference can be generated using the model inverse of equation (11). First, the feed forward input ($T_{c2,ff}$) of clutch torque can be calculated through dynamics of $x_3 = T_o$ and $T_{o,d}$.

$$T_{c2,ff} = \frac{J_{ct2,eq}}{c_{o,eq} r_2 f r_2} \Big\{ \dot{T}_{o,d} - k_{o,eq} x_{2,ff} + c_{o,eq}\Big(\frac{1}{J_{ct2,eq}} + \frac{1}{J_v}\Big) T_{o,d} \Big\} \tag{17}$$

where, since $x_{2,ff}$ is the compliance of the output shaft, it is calculated using output shaft modeling and $T_{o,d}$.

$$x_{2,ff} = -\frac{\dot{T}_{o,d}(t_0) - k_{o,eq} x_2(t_0)}{k_{o,eq}} e^{-\frac{k_{o,eq}}{c_{o,eq}}(t - t_0)} + \frac{\dot{T}_{o,d}}{k_{o,eq}} \tag{18}$$

Second, $T_{in,ff}$ is calculated using dynamics of $x_1 = \omega_{slip}$, $T_{o,d}$, $T_{c2,ff}$ and $\omega_{slip,d}$.

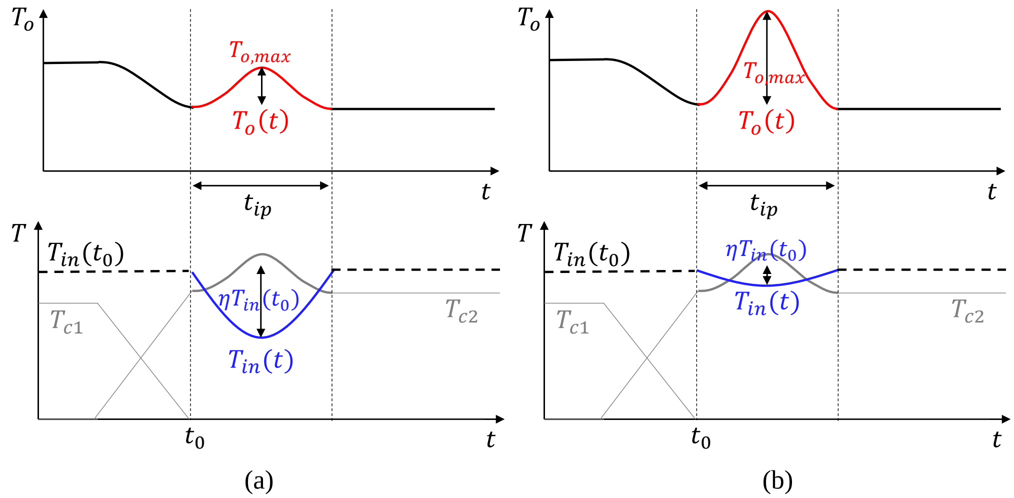

Figure 4: Figure showing the proposed reference planning method. (A): Increased eta to reduce the jerk of drive torque. (Comfort mode) / (b): Reduced eta to increase the maximum drive torque. (Sports mode)

$$T_{in,ff} = J_{in}\Big\{\dot{\omega}_{slip,d} + \Big(\frac{1}{J_{in}} + \frac{(r_2 fr_2)^2}{J_{ct2,eq}}\Big)T_{c2,ff} - \frac{r_2 fr_2}{J_{ct2,eq}}T_{o,d}\Big\} \quad (19)$$

Multivariable Controller Design

This paper targets an electrified vehicle with a multivariable controller for DCT gear shift. In this system, there are various system uncertainties such as nonlinearity of clutch disk friction coefficient, load torque (T_v), and gear back lash. To be robust against this uncertainty, a robust shift controller such as the H_∞ control method is used [1]. In addition, a loop shaping technique that allows convenient control gain tuning and adjusts the frequency response of a closed loop system is also used [5]. Therefore, in this paper, H_∞ loop shaping controller that is robust to uncertainty and can adjust the frequency response was selected.

The desired plant transfer function (G_d) must be designed for loop shaping. For this, it is necessary to analyze the dominant disturbance of the system. Disk friction coefficient and load torque mainly have a frequency band of 0 to 5Hz. Encoder noise and load noise have a bandwidth of 1kHz or higher. Therefore, the desired plant transfer function was designed to have a 5Hz cutoff frequency (ω_c). (Fig. 6)

To design the controller, the powertrain modeling of the electrified vehicle shown in equation (11) can be converted to a transfer function through $G(s) = C(sI - A)^{-1}B + D$.

For shaping G with G_d, the stable minimum phase filer W can be designed using the greatest common division formula [11]. The nominal shaped plant (G_s) multiplied by W and plant can be expressed as normalized left coprime factorization as follows.

$$G_s = WG = M^{-1}N \quad (20)$$

G_s can be expressed as perturbed shaped plant ($G_{s\Delta}$) including model uncertainties.

$$G_{s\Delta} = \left\{(M + \Delta_M)^{-1}(N + \Delta_N) : \| \begin{bmatrix}\Delta_M & \Delta_N\end{bmatrix} \|_\infty < \epsilon\right\} \quad (21)$$

where, Δ_M and Δ_N indicate model uncertainties, and $\|\cdot\|_\infty$ means H_∞ norm. In addition, $\epsilon > 0$ represents the H_∞ bound of model uncertainties. For G_s with feedback controller K_∞ is robust stable if and only if G is stable and

$$\gamma = \min_{K_\infty} \left\| \begin{bmatrix} I \\ K_\infty \end{bmatrix} (I - G_s K_\infty)^{-1} \begin{bmatrix} G_s & I \end{bmatrix} \right\|_\infty < \epsilon^{-1}. \quad (22)$$

where, γ is a suboptimal solution that satisfies the above equation [12]. Finally, the stabilizing controller K can be expressed as $K = WK_\infty$.

As can be seen in the singular value plot (Fig. 7) of the open loop and closed loop transfer functions of G with stabilizing controller K, a shaped plant can be obtained that matches the desired plant.

Verification with Simulation

In order to verify the reference planning method and the feed forward input generation method proposed in this paper, an electrified vehicle with DCT was constructed and a shift controller suitable for this was designed with SimDriveline of MATLAB/SIMULIK. At this time, the specifications of the target vehicle are shown in the following table.

Table 1: Table of target vehicle spec.

Name	Value
Mass	$1400kg$
Max.power source torque	$250Nm$
Transmission	2-speed DCT
First gear ratio (r_1)	3.85
Second gear ration (r_2)	2
Final gear ratio 1 (fr_1)	4
Final gear ratio 2 (fr_2)	4.17
Power source inertia (J_{in})	$0.22kg \cdot m^2$
Equivalent clutch 2 inertia ($J_{c2,eq}$)	$2.60kg \cdot m^2$
Vehicle inertia (J_v)	$144.52kg \cdot m^2$

In the simulation scenario, an upshift that shifts from first to second gear is assumed. Shift schedular provides η and t_{ip} to the shift controller according to the driving mode. Using this, the reference planer creates a reference for the output variable and a feed forward input. In parallel, a multivariable controller with tracking error as

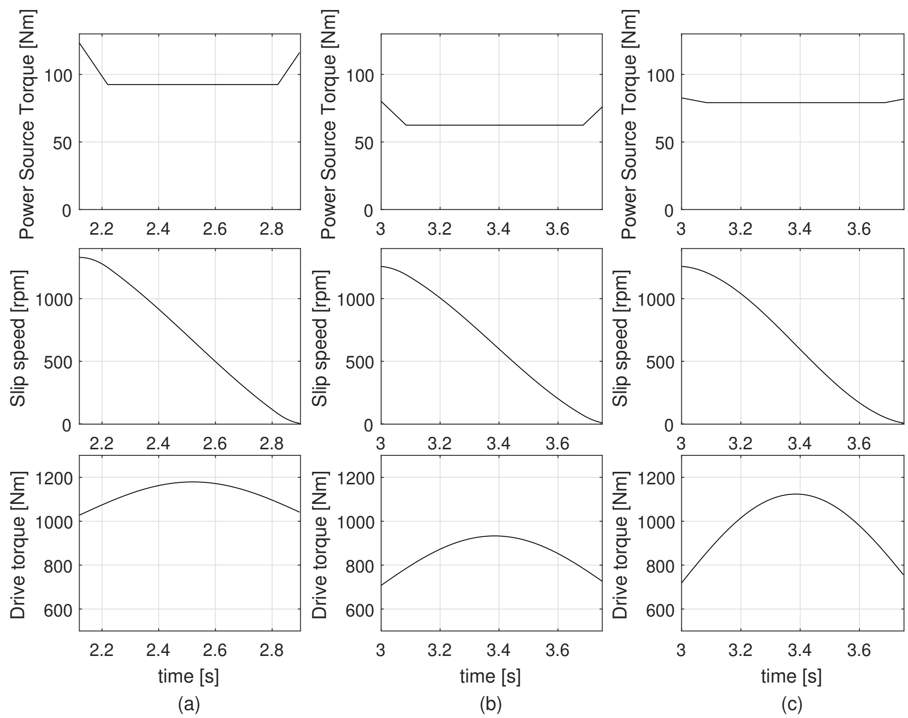

Figure 5: Example of reference created using the proposed reference planning method. (a): $T_{in}(t_0) = 123Nm$, $\eta = 0.25$, $t_{ip} = 0.8s$ /(b): $T_{in}(t_0) = 81Nm$, $\eta = 0.25$, $t_{ip} = 0.8s$ /(c): $T_{in}(t_0) = 81Nm$, $\eta = 0.05$, $t_{ip} = 0.8s$

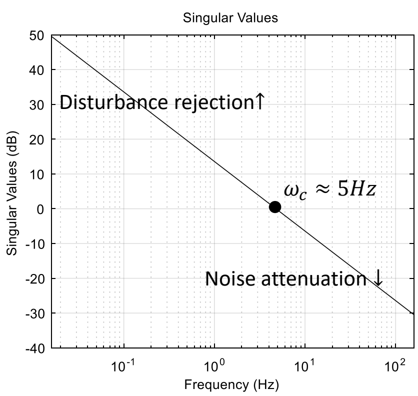

Figure 6: Frequency response of desired plant (G_d)

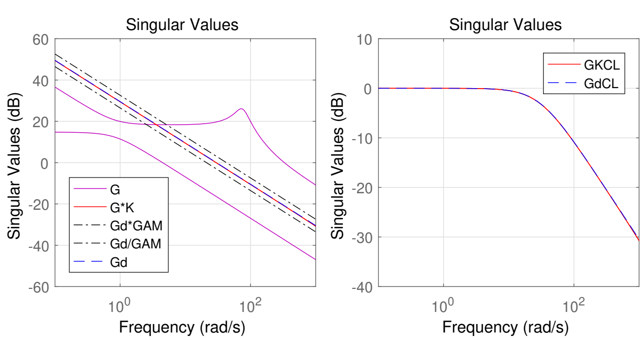

Figure 7: Frequency response of original, desired, shaped and closed loop transfer function.

input creates feedback input. The control diagram from the driver input to the shift controller is shown in the Fig. 8.

Since the proposed method in this paper is an improved control method for the reference planer, in simulation, the heuristic reference planning method proposed in the previous research [5] is implemented together to compare shift control performance. In this case, it is assumed that the η and t_{ip} of the scheduler generated from the driver input is 0.25 and 0.8 seconds, respectively.

The two types of references made in the same situation are shown in the Fig. 9. Here, the drive torque was generated based on $sin(t)$ to have a smooth shape.

Referring to the Fig. 9, you can see that it has a smaller $T_{o,max}$ than the reference created by using previous research. This result means that a drive torque reference with a lower jerk was created. In addition, it can be seen that the slip speed reference has a different shape from the result of previous research.

Except for the reference planer and feed forward controller, the results when shift control was performed with the same shift controller were plotted in the Fig. 10. In particular, the controller was tuned to have the same squared jerk integral to calculate the control input effort used in the inertia phase. Shift control performance is shown in the Table. 2.

Table 2: Table of shift control performance.

Performance Name	Previous	Proposed
Reference planning method	Hand tuning	Automatic
$\int u_{FB}^2 dt$	294.73	264.45 (10.3% ↓)
$\int jerk^2 dt$	127.81	127.94

In both cases, there was no difference in tracking performance, but there was a performance difference due to the reference difference. First, the reference generated from the previous research results required tuning for each shift scenario, but the reference generated using the proposed method can be automatically generated according to the driving mode. Second, when comparing the integral values of the squared feedback input, a control input reduction effect of about 10% can be obtained.

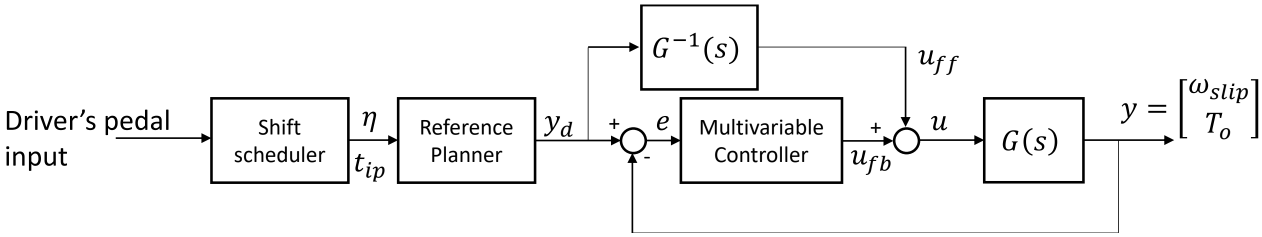

Figure 8: DCT shift control schematic diagram using the proposed reference planning method.

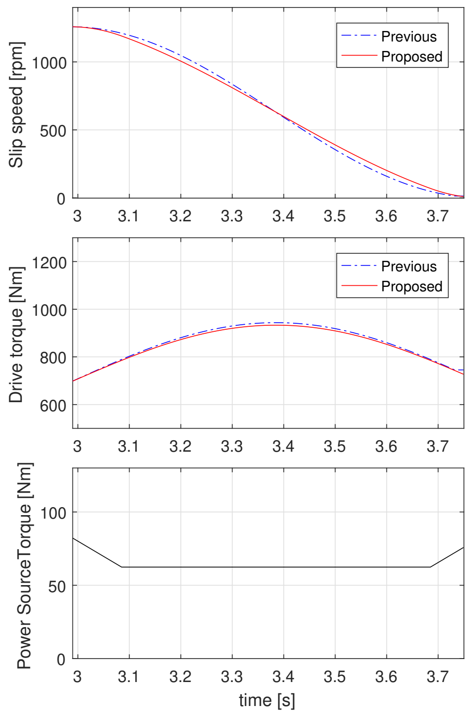

Figure 9: Comparison of proposed reference planning method with previous research method. The same power source input, but different references are created. For the slip speed reference, the shape was changed.

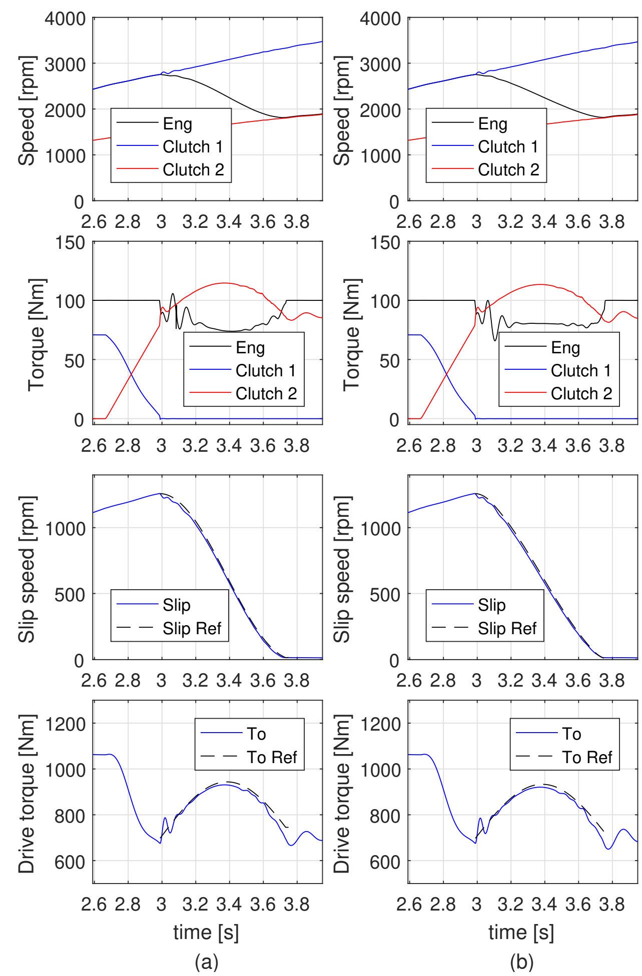

Figure 10: The result of applying the proposed reference planning method (b) and the method of the previous study (a) through simulation and performing shift control. Despite the flat shape power source input, more feedback input was generated for reference planning using previous research.

Conclusion and Future Work

In this paper, to maximize acceleration performance and energy efficiency of electrified vehicles, a reference planning method of slip speed and drive torque of a multivariable controller targeting a DCT-equipped powertrain is presented. In the previous study, since slip speed and drive torque reference were generated in a heuristic method, tuning was necessary for every shift scenario, and unnecessary control inputs and jerks could increase. However, this study proposed a method for generating a reference that satisfies power train dynamics. In addition, if multivariable control is performed using this method, automatic reference generation using the initial state is possible, and approximately 10% less feedback input is used. It was also verified through simulation that the same shift performance can be obtained.

Minimizing the feedback input through the proposed reference planning method can reduce the feedback gain and increase the stability margin of the closed loop system. By using the method in which the reference is automatically generated, it is possible to reduce the cost required for tuning and increase the transmission performance. Since energy consumption of the power source and clutch actuator can be reduced, the overall energy efficiency of the vehicle can be improved. As an energy efficiency improvement effect, HEV can improve fuel efficiency and EV can improve electrical efficiency. In addition, the reference planning method proposed in this paper is widely applicable to electrified vehicles. If an input constraint is considered, it can be applied to conventional vehicles where ICE is a power source.

The method proposed in this paper cannot be reflected in reference planning in real time if η and t_{ip} generated from the driver's pedal input change during shifting. However, since t_{ip} is usually set to 0.5 to 1 second, the pedal input of the driver can be changed sufficiently during shifting. Therefore, it is necessary to further study the reference planning method considering η and t_{ip} changes in the inertia phase. Specifically, when changing the reference in real time, the reference is continuously connected using the current slope and the final target value, and the control input is minimized by considering powertrain dynamics. Using this method, the reference planning method proposed in this paper can be improved.

References

1. Z.-G. Zhao, H.-J. Chen, Y.-Y. Yang, and L. He, "Torque coordinating robust control of shifting process for dry dual clutch transmission equipped in a hybrid car," *Vehicle System Dynamics*, vol. 53, no. 9, pp. 1269–1295, 2015.

2. P. Walker, B. Zhu, and N. Zhang, "Powertrain dynamics and control of a two speed dual clutch transmission for electric vehicles," *Mechanical Systems and Signal Processing*, vol. 85, pp. 1–15, 2017.

3. S. Hong, S. Ahn, B. Kim, H. Lee, and H. Kim, "Shift control of a 2-speed dual clutch transmission for electric vehicle," in *2012 IEEE Vehicle Power and Propulsion Conference*, pp. 1202–1205, IEEE, 2012.

4. Z. Lei, D. Sun, Y. Liu, D. Qin, Y. Zhang, Y. Yang, and L. Chen, "Analysis and coordinated control of mode transition and shifting for a full hybrid electric vehicle based on dual clutch transmissions," *Mechanism and Machine Theory*, vol. 114, pp. 125–140, 2017.

5. S. Kim and S. B. Choi, "Cooperative control of drive motor and clutch for gear shift of hybrid electric vehicles with dual-clutch transmission," *IEEE/ASME Transactions on Mechatronics*, 2020.

6. M. Roozegar and J. Angeles, "Gear-shifting in a novel modular multi-speed transmission for electric vehicles using linear quadratic integral control," *Mechanism and Machine Theory*, vol. 128, pp. 359–367, 2018.

7. M. Roozegar and J. Angeles, "The optimal gear-shifting for a multi-speed transmission system for electric vehicles," *Mechanism and Machine Theory*, vol. 116, pp. 1–13, 2017.

8. B. Alt, F. Antritter, F. Svaricek, and M. Schultalbers, "Multivariable speed synchronisation for a parallel hybrid electric vehicle drivetrain," *Vehicle System Dynamics*, vol. 51, no. 3, pp. 321–337, 2013.

9. Q. Ren, D. Crolla, and A. Morris, "Effect of transmission design on electric vehicle (ev) performance," in *2009 IEEE vehicle power and propulsion conference*, pp. 1260–1265, IEEE, 2009.

10. T. Hofman and C. Dai, "Energy efficiency analysis and comparison of transmission technologies for an electric vehicle," in *2010 IEEE vehicle power and propulsion conference*, pp. 1–6, IEEE, 2010.

11. V. Le and M. Safonov, "Rational matrix gcds and the design of squaring-down compensators-a state-space theory," *IEEE Transactions on Automatic Control*, vol. 37, no. 3, pp. 384–392, 1992.

12. K. Glover and D. McFarlane, "Robust stabilization of normalized coprime factor plant descriptions with h/sub infinity/-bounded uncertainty," *IEEE transactions on automatic control*, vol. 34, no. 8, pp. 821–830, 1989.

Acknowledgments

This work was supported by the National Research Foundation of Korea(NRF) grant funded by the Korea government(MSIP) (No. 2020R1A2B5B01001531), and the BK21+ program through the NRF funded by the Ministry of Education of Korea.